39th AIAA/ASME/SAE/ASEE Joint Propulsion Conference and Exhibit
20-23 July 2003, Huntsville, Alabama

AIAA 2003-5155

THE EFFECTS OF CLUSTERING MULTIPLE HALL THRUSTERS ON PLASMA PLUME PROPERTIES

Brian E. Beal* and Alec D. Gallimore†
Plasmadynamics and Electric Propulsion Laboratory
Department of Aerospace Engineering
The University of Michigan
Ann Arbor, MI 48109 USA

William A. Hargus, Jr.‡
Air Force Research Laboratories
Edwards Air Force Base
Edwards, CA 93524 USA

ABSTRACT

Clusters of Hall thrusters have been proposed as a means of achieving electric propulsion systems capable of operating at very high power levels. To facilitate testing in existing vacuum facilities, initial tests have focused on a cluster of low-power Busek BHT-200-X3 Hall thrusters. A combination of triple Langmuir probes and floating emissive probes is used to study the effects of multi-thruster operation on the electron number density, electron temperature, and plasma potential in the plasma plume. The resultant number density is shown to be a result of linear superposition of the plumes of individual thrusters, while the electron temperature in the cluster plume is measured to be slightly higher than that caused by operation of a single thruster. The plasma potential downstream of the cluster is shown to obey the Boltzmann relation. In the region between the thrusters, the plasma potential increases as a function of downstream distance and may result in reflection of some low-energy charge exchange ions back toward the cluster. A mechanism that may lead to slightly reduced ion beam divergence through focusing of ions directed toward the thruster centerline is discussed.

Introduction

Both NASA and the United States Air Force (USAF) are conducting research into electric propulsion (EP) systems operating at power levels in excess of 100 kW. The Air Force will use high-power systems for orbit transfer vehicles and rescue vehicles capable of repositioning assets that have exhausted their propellant load or failed to meet their operational orbit.[1,2] NASA predicts that high-power EP systems will be used in both a high thrust mode to reduce mission times and in a high specific impulse mode to enable deep space missions that require high velocity increments (ΔV).[3,4] NASA's recently announced Project Prometheus will seek to develop space nuclear reactors capable of meeting the power demands of in-space propulsion.[5] The commencement of this project increases the likelihood that high-power EP systems will become viable for deep space missions where the availability of solar power is diminished, as well as for the near-Earth missions of interest to the Air Force.

One electric propulsion device that is of interest for each type of mission discussed above is the Hall thruster due to its low specific mass, high thrust density, and high reliability. Although the envisioned power level is somewhat beyond the current state-of-the-art, there are two approaches being considered for reaching high powers. The first, known as the monolithic approach, is to design a single thruster capable of operating at the desired power level. The second, complementary approach involves clustering several moderately powered thrusters together to reach the desired power level.

The clustered approach, which is the one being pursued by the USAF, may be expected to have a slightly lower total efficiency and higher dry mass than a comparable monolithic device since large thrusters have historically outperformed smaller thrusters. A cluster of thrusters, however, has several advantages over a single unit including

* Ph.D Candidate, Student Member AIAA
† Associate Professor, Associate Fellow AIAA
‡ Research Scientist, Senior Member AIAA

improved system reliability and the ability to throttle the system by simply turning on or off the appropriate number of thrusters. Throttling the system in this way allows a cluster to perform at lower powers without operating any of the individual thrusters at off-design conditions. This characteristic of a cluster may prove beneficial on missions where either the available power or the propulsive needs change as a function of time. For example, a high-power cluster of Hall thrusters could be used for the initial LEO-GEO transfer of a geosynchronous communications satellite. Upon reaching its final destination, one element of the cluster could then be used for north-south station keeping. A final, very important advantage of operating multiple thrusters is the high degree of system scalability. In principle, once the technical issues involved with operating a cluster are understood, a single flight-qualified engine could support a wide range of missions by simply clustering together the appropriate number of thrusters.

Before a cluster of Hall thrusters can be used in flight, there are several technical issues that must be addressed.[1,2] One of the most pressing issues is the need to understand the interaction of the plasma plumes with each other and with the spacecraft. In an effort to address this issue, testing of four 200-watt Busek BHT-200-X3 thrusters has begun at both the Air Force Research Laboratory (AFRL) and at the University of Michigan's Plasmadynamics and Electric Propulsion Laboratory (PEPL).[6-8] Figure 1 shows the cluster in operation at AFRL.

Figure 1: A low-power Hall thruster cluster in operation.

The current work focuses on determining the relations necessary to predict the plume properties of a cluster based on measurements or simulations of a single thruster plume. To this end, the plume of the cluster is characterized using a combination of electrostatic triple probes and emissive probes to measure the electron number density, electron temperature and plasma potential. In addition, a three-axis gaussmeter is used to measure the magnetic field downstream of the cluster.

Experimental Setup

Cluster

The cluster used in this experiment is composed of four Busek BHT-200-X3 200-watt class Hall thrusters. An earlier version of this thruster is reported to operate at an anode efficiency of 42% and specific impulse of 1300 seconds while providing 12.4 mN of thrust at the nominal operating conditions.[9] Each thruster has a mean diameter of 21 mm. The thrusters are arranged in a 2x2 grid with approximately 11.4 centimeters between the centerlines of adjacent thrusters. Typical operating conditions for the BHT-200 are given in Table 1.

Parameter	Value
Discharge Voltage (V)	250 ± 0.5
Discharge Current (A)	0.80 ± 0.03
Cathode Voltage (V)	-8.5±1.0
Magnet Current (A)	1.0 ± 0.03
Keeper Current (A)	0.5 ± 0.05
Keeper Voltage (V)	13 ± 1
Anode Mass Flow (sccm)	8.5 ± 0.85
Cathode Mass Flow (sccm)	1.0 ± 0.1

Table 1: Typical thruster operating conditions.

Vacuum Chamber

All data reported in this paper are recorded in Chamber 6 at AFRL. Chamber 6 is a 1.5 x 2.4 meter cylindrical, stainless steel vacuum chamber that is evacuated by four cryopanels maintained at 25 Kelvin by four APD cold heads, HC-8C helium compressors, and an APD cryopump.[10] This system provides a pumping speed of 26,000 liters per second of xenon with a typical base pressure of 8×10^{-7} Torr as measured by a MKS Model 910 hot cathode gauge. During thruster operation, the chamber pressure rises to approximately 6.1×10^{-6} Torr for single thruster operation and 2.3×10^{-5} Torr for four-thruster operation. Both reported pressures are corrected for xenon.

Positioning System and Nomenclature

The naming convention and coordinate system used throughout this experiment are shown in Fig. 2. As shown, the thrusters are labeled as TH 1-4 beginning in the upper left-hand corner and proceeding counterclockwise. The origin of the coordinate system is defined as the midpoint of the cluster in the displayed X-Y plane. The Z coordinate measures the distance downstream of the thruster exit plane.

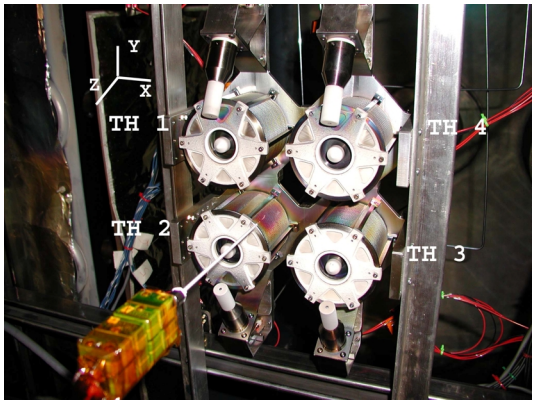

Figure 2: Cluster nomenclature and coordinate system.

A three-dimensional positioning system is used to sweep probes through the cluster plume. The X and Z positions are adjusted using a single two-axis Parker Daedal table with approximately 30 cm of travel in each direction. The Y position is controlled using a vertically mounted Parker Daedal linear stage with a 45 cm range of motion.

Triple Probe

The triple Langmuir probe used for these experiments consists of 3 tungsten electrodes insulated from each other by an alumina rod. Each electrode is 0.5 mm (0.020") in diameter and 5.0 mm (0.20") long. The spacing between the centerlines of adjacent electrodes is approximately 2 mm. The probe is sized to criteria that allow the standard "thin sheath" assumptions of probe theory to be applied.[11] These criteria, which are discussed elsewhere,[6] are necessary to ensure proper operation of the probe.

The symmetric triple probe, originally developed by Chen and Sekiguchi,[12] is a convenient plasma diagnostic for collecting large amounts of data due to the elimination of the voltage sweep required by other electrostatic probes. Additionally, since the probe as a whole floats, the disturbance to the ambient plasma is minimized compared to single probes, which draw a net current from the discharge. A schematic of the triple probe circuit is shown in Fig. 3. As shown in this diagram, electrode 2 is allowed to float while the voltage between electrodes 1 and 3, V_{d3}, is applied by a laboratory power supply with floating outputs. For the experiments discussed here, V_{d3} is set to 12 volts. The potential between probes 1 and 2, V_{d2}, is measured by an HP 34970A data acquisition system, as are the floating potential, V_f, and the current, I.

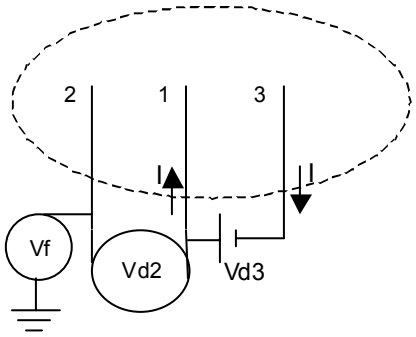

Figure 3: Triple probe circuit.

The relations used to determine plasma properties from measured probe data are presented in Eqn. 1 and 2. In these equations, n_e is the electron number density, which is equal to the ion number density through the quasineutrality assumption. The electron temperature is represented by T_e and ion and electron masses by m_i and m_e, respectively. The symbol A denotes the area of a single electrode, e is the electron charge, and k_b is Boltzmann's constant. Various error analyses indicate that the uncertainty in the calculated electron temperature and number density are generally less than 30% and 50%, respectively.[12-13] The relative uncertainty between multiple data points recorded using the same probe is believed to be significantly lower than the absolute uncertainty.

$$n_e = \left(\frac{em_i}{k_b T_e}\right)^{1/2} \frac{I \exp\left(\frac{1}{2}\right)}{Ae^{3/2}\left[\exp\left(\frac{eV_{d2}}{k_b T_e}\right) - 1\right]} \qquad (1)$$

$$\frac{1 - \exp\left(\frac{-eV_{d2}}{k_b T_e}\right)}{1 - \exp\left(\frac{-eV_{d3}}{k_b T_e}\right)} = \frac{1}{2} \qquad (2)$$

Emissive Probe

Plasma potential measurements are conducted using a floating emissive probe similar to the one described by Haas *et al*.[14] The emitting portion of the probe consists of a 0.127 mm (0.005") diameter tungsten filament loop, the ends of which are inserted into double bore alumina tubing along with 0.508 mm (0.020") diameter molybdenum wire leads. Short lengths of tungsten wire are inserted into the alumina tube to insure contact between the emitting filament and molybdenum leads. The diameter of the emitting filament loop is approximately 3 mm. Figure 4 shows a sketch of the emissive probe.

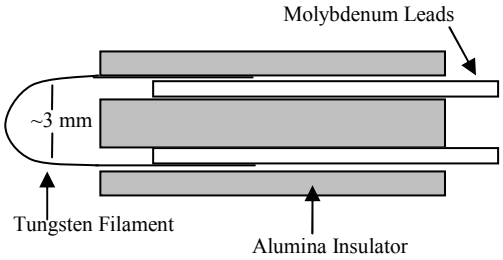

Figure 4: A schematic of the emissive probe.

The theory of the emissive probe is well established and results in the conclusion that a thermionically emitting filament will assume the local plasma potential when its emitted electron current is sufficient to neutralize the plasma sheath.[15] For this experiment, the current necessary to heat the probe is provided by a programmable Sorensen model DLM 40-15 power supply with floating outputs. At each location in the plume, the current is steadily increased and the potential with respect to ground at the negative terminal of the supply is recorded using the HP data acquisition unit mentioned above. This method allows for verification of a well-defined plateau in the voltage-current trace, which indicates plasma sheath neutralization. The shape of a typical trace, such as the one shown in Fig. 5, can be explained as follows. At zero applied current, the probe assumes the local floating potential. As the current to the probe is increased, the measured potential initially decreases as a voltage appears across the probe and causes the potential at the negative terminal to move below the floating potential. As the probe current is increased further, the filament begins to emit electrons causing the measured potential to rise sharply before approaching an asymptote at the local plasma potential. Considering that the voltage drop across the emitting filament never exceeds 6 V, the uncertainty in the plasma potential measurements is estimated to be ±3 V.

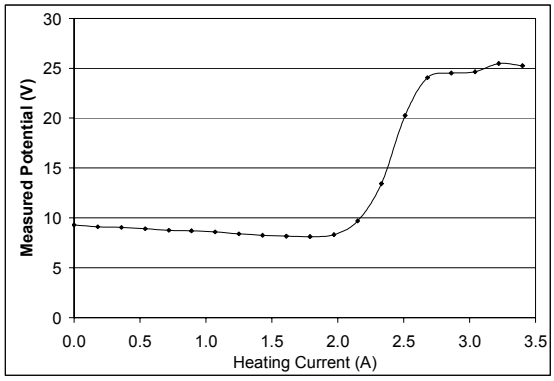

Figure 5: Sample emissive probe trace.

Gaussmeter

The magnetic field downstream of the cluster is recorded using an FW Bell model 7030 three-axis gaussmeter. All measurements are recorded without the thrusters in operation. Although recent work has shown the magnetic field strength profiles inside an operating thruster to deviate from the applied profiles due to fields induced by the azimuthal electron drift,[16] the difference is expected to be negligible for the low-power thrusters studied here because of the low current levels involved. The magnetic field profiles presented in this paper are therefore believed to be realistic representations of those that occur downstream of an operational cluster.

Results and Discussion

Magnetic Field

Magnetic field data are recorded in the XZ plane of thrusters 2 and 3, and in the YZ plane of thrusters 3 and 4. The results are shown in Figs. 6 and 7, respectively. The differences in these plots are attributable to the different direction of magnet current flow between thrusters 2 and 4. Thrusters 2 and 3 are operated with the electromagnets in the nominal configuration while the current flow was reversed in thruster 4. Reversing the polarity of electromagnets in alternate thrusters of a cluster has been suggested as a means of canceling the disturbance torques that typically result from the slight ExB drift of the beam ions.[1,2,17] The data presented in Figs. 6 and 7 will be used to test the previously published theory that the plasma potential profiles of a cluster can be predicted from magnetic field data.[8]

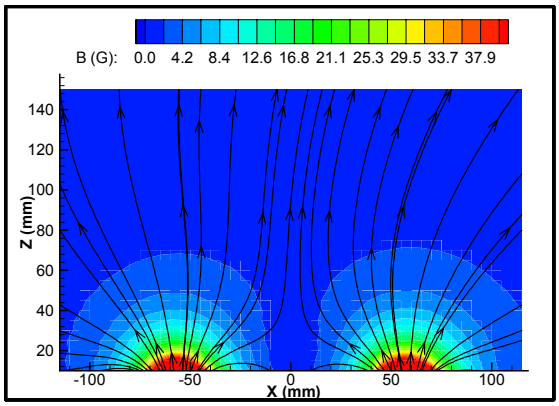

Figure 6: The magnetic field strength and streamtraces downstream of TH 2 & 3.

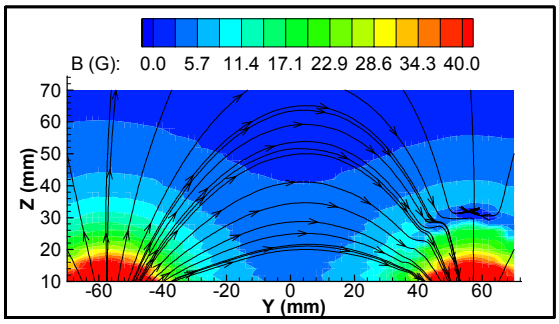

Figure 7: Magnetic field profiles downstream of thrusters 3 & 4. The polarity of magnet 4 has been reversed from the normal configuration.

Plasma Density

A triple Langmuir probe is used to measure the plasma number density at 5 mm intervals in the cluster plume. Data are recorded in both the XZ plane of thrusters 2 and 3 and the YZ plane of thrusters 3 and 4. For both planes, data are recorded with each thruster operating alone and with two thrusters operating simultaneously. Due to the good agreement between the two data sets, only the data recorded in the YZ plane of thrusters 3 and 4 are reported here.

The plasma density profiles downstream of thrusters 3 and 4 are shown in Fig. 8. As this plot shows, the maximum number density 50 mm downstream of the cluster exit plane is roughly $1x10^{18}$ m^{-3}. This value decreases rapidly in the downstream direction and by Z=250 mm the maximum plasma density has decreased by more than an order of magnitude to about $5x10^{16}$ m^{-3}. Figure 8 shows a well-defined jet structure downstream of each individual thruster. By about 250 mm downstream the plumes have merged to the point that the density is nearly constant across the width of the cluster and resembles the profile that would be expected downstream of a large monolithic thruster.

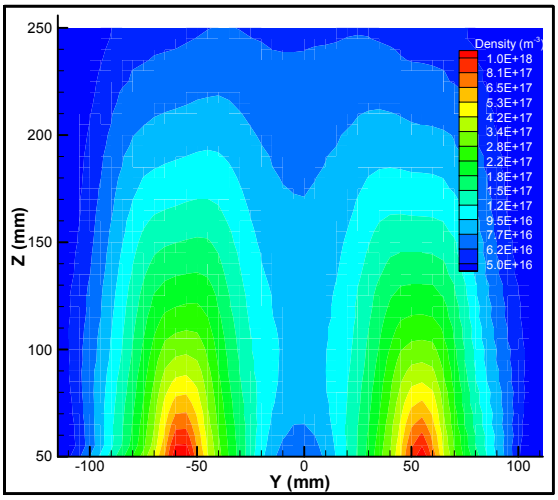

Figure 8: Electron number density in the plume of thrusters 3 and 4.

Figures 9-11 show plasma density profiles at axial distances of 50, 150, and 250 mm downstream of the cluster exit plane. The black lines in these plots are obtained by linear superposition of the data recorded with thruster 3 and thruster 4 running independently. The measurements of plasma density taken with both thrusters operating simultaneously agree with the calculated values to well within the margin of error of the triple probe diagnostic. This implies that the density in a cluster plume, n, can be predicted by summing the contributions of each individual thruster, n_j, as shown in Eqn. 3.

$$n = \sum_j n_j \qquad (3)$$

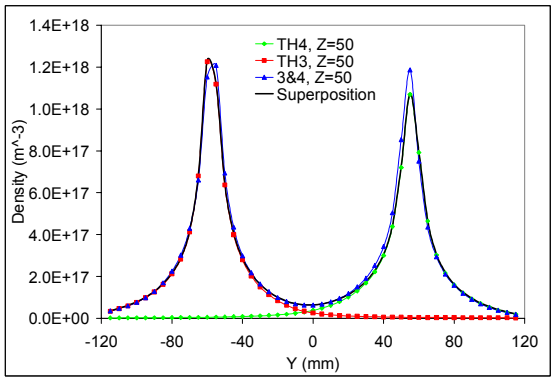

Figure 9: Plasma density at Z=50 mm. The data show good agreement with linear superposition.

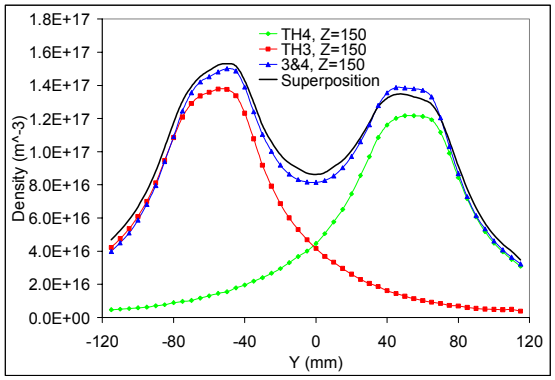

Figure 10: Plasma density at z=150 mm.

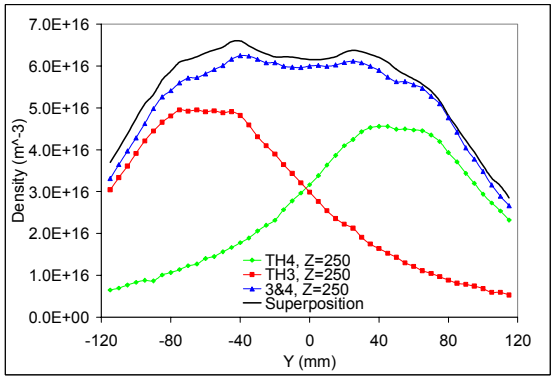

Figure 11: Plasma density at z=250 mm.

Electron Temperature

The electron temperature contours recorded downstream of thrusters 3 and 4 are displayed in Fig. 12. The temperature varies between roughly 3 eV at Z=50 mm along the thruster centerlines to less than 1 eV near the boundaries of the sampled region. The data show slight discrepancies in the electron temperature in the near-field of each individual thruster. Measurements recorded downstream of thrusters 2 and 3 (not shown) indicate similar differences, thus the variations are not believed to be a result of the reversed magnetic field profiles mentioned previously. Rather, the discrepancies are probably due to tolerances in the manufacturing process or differences in the cumulative time of operation between the devices. The difference in the electron temperature in front of each thruster decreases as a function of downstream distance and by roughly Z=90 mm the difference between the two units becomes negligible.

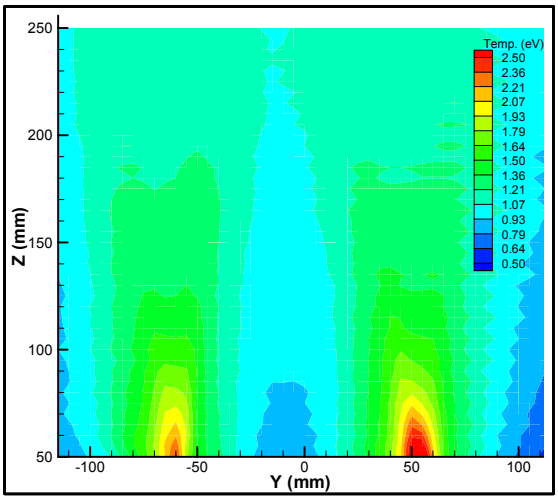

Figure 12: Electron temperature profiles downstream of thrusters 3 and 4.

Electron temperature traces measured at axial locations of 50, 150, and 250 mm are shown in Figs. 13-15, respectively. The black line in each figure is calculated using Eqn. 4 and represents a first attempt to predict the electron temperature in the cluster plume. The simplistic approach of calculating a density weighted average, as indicated by Eqn. 4, seems to slightly underpredict the measured temperature, particularly in the region between the thrusters. The electron temperatures measured during thruster operation are consistently higher than those recorded during single thruster operation; however the difference is generally less than 0.2 eV, which is within the uncertainty of the diagnostic.

$$\frac{k_b T_e}{e} = \frac{\sum_j n_j \frac{k_b T_{ej}}{e}}{\sum_j n_j} \qquad (4)$$

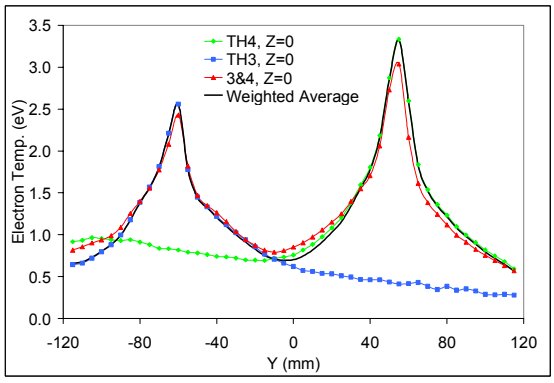

Figure 13: The electron temperature profiles measured for single- and multi-thruster operation 50 mm downstream of the exit plane.

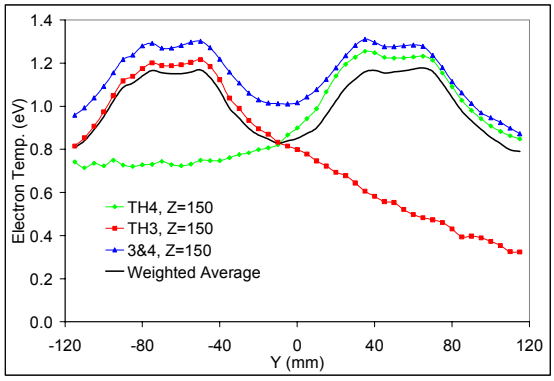

Figure 14: Electron temperature profiles 150 mm downstream of the cluster exit plane.

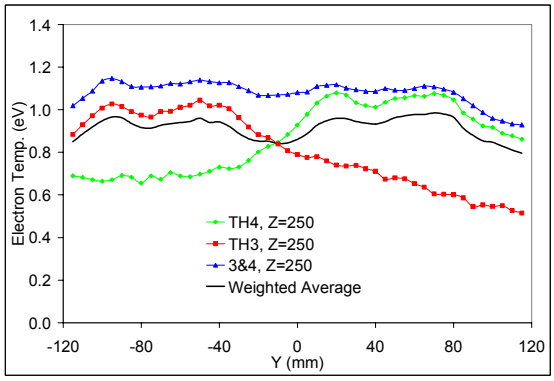

Figure 15: The electron temperature 250 mm downstream of the thrusters.

Plasma Potential

An emissive probe is used to measure the plasma potential at 5 mm intervals in the cluster plume. Results obtained with thrusters 3 and 4 operating simultaneously are shown in Fig. 16. An interesting feature shown in this plot is the unique plasma potential profile in the area between the thrusters. Between approximately Y=-30 and Y=30 mm, the plasma potential increases with downstream distance indicating that there exists a region where the electric field vector is oriented in the upstream direction. This can be seen clearly in Fig. 17, which shows the plasma potential profiles at various axial locations. The reversed electric field could potentially cause ions produced in the area between the thrusters to be accelerated upstream toward the spacecraft on which the thrusters are mounted. Although this could result in an increased erosion rate in some areas due to increased ion impingement, the effect is expected to be negligible since the impinging ions are unlikely to experience accelerating potentials greater than a few volts in the reverse direction.

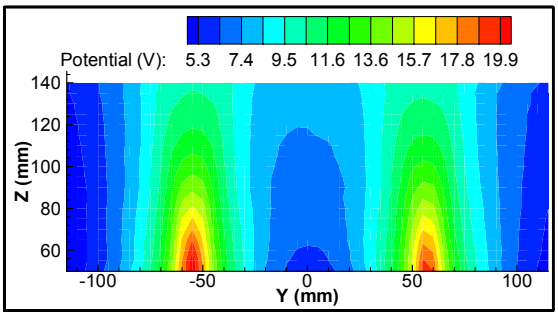

Figure 16: Plasma potential profiles downstream of thrusters 3 and 4.

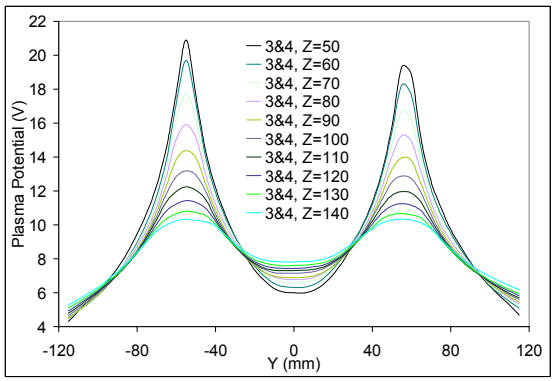

Figure 17: The evolution of plasma potential profiles at various downstream locations.

It has been suggested that the plasma potential profiles downstream of a cluster could be predicted by simply integrating the magnetic field data.[8] This is contradicted by the measurements presented in Figs. 18-20, which show the plasma potential downstream of thrusters 3 and 4 at axial distances of 60, 100, and 140 mm, respectively. Clearly, integration along the magnetic field lines depicted in Fig. 7 does not result in the observed potential profiles.

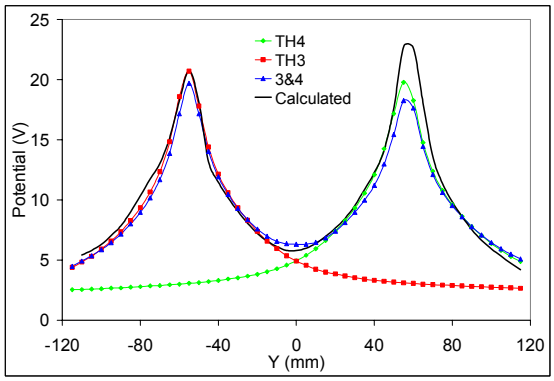

Figure 18: Plasma potential measured 60 mm downstream of the cluster exit plane using a floating emissive probe.

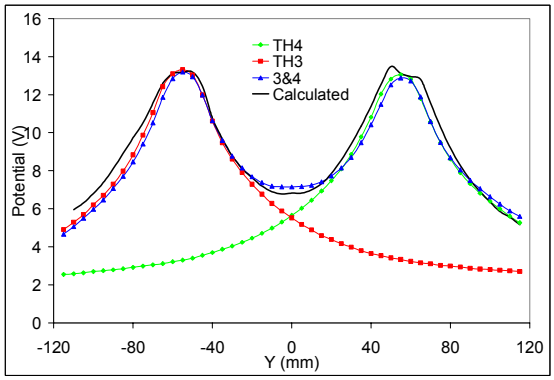

Figure 19: Plasma potential profiles 100 mm downstream of thrusters 3 and 4.

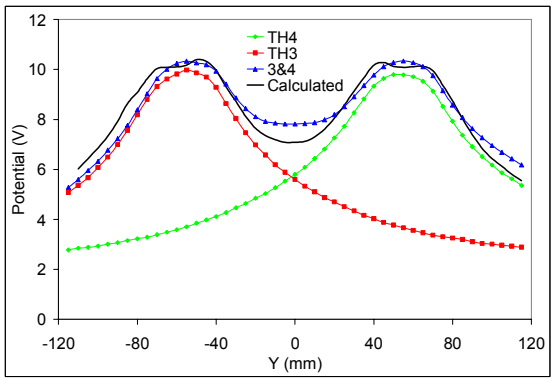

Figure 20: Plasma potential measured 140 mm downstream. Note the agreement between measured values and those calculated using the Boltzmann equation.

A more conventional method for relating the magnetic field architecture to the plasma potential involves consideration of electron dynamics in a plasma. Along a magnetic field line, the motion of electrons is governed purely by electrostatic forces and can be described by the well known Boltzmann relation.[18] This leads naturally to the definition of a thermalized potential, ϕ_T, which is conserved along a line of force.[19] The thermalized potential is defined by Eqn. 5 where ϕ represents the plasma potential and n_0 is a reference density taken at some point along the field line. In the derivation of Eqn. 5, the electron temperature has been assumed constant along lines of force.

$$\phi_T \equiv \phi - \frac{k_B T_e}{e} \ln\left(\frac{n}{n_0}\right) \qquad (5)$$

The concept of thermalized potential is useful in the design of Hall thrusters since it shows that the magnetic field lines can be approximated as equipotential lines in situations where the electron temperature is negligible compared to the plasma potential. In other words, the thermalized potential is a useful tool for predicting plasma potential in situations where electrons are tightly bound to the magnetic field lines. This method, however, is less useful in the thruster plume since the correction term due to thermal effects and density gradients can be as large as the plasma potential.

Comparing the plasma potential data of Fig. 16 to the magnetic field profiles shown in Fig. 7, it is clear that the lines of force do not correspond to equipotential contours. This is not surprising, since the magnetic field strength is generally less than 10 G and the electrons are only weakly magnetized throughout the areas where the plasma potential is presented. In this situation, thermal effects and density gradients are dominant over the effects of the magnetic field, and the plasma potential is described by the Boltzmann equation given by Eqn. 6. The profiles calculated using Eqn. 6 are shown in Figs. 18-20 and generally agree to within one volt of the measured values, except in the most upstream locations of the sampled region. In utilizing Eqn. 6, the reference density (n_0=7x10^{17} m^{-3} in this case) is chosen so as to make the plasma potential calculated along the centerline of thruster 3 at 100 mm match the measured value. While the choice to match the value at 100 mm is arbitrary, this approach is expected to be valid in most practical cluster configurations since the data presented here shows the plasma potential directly downstream of one thruster in a cluster to be largely unaffected by the surrounding devices. Implementation of Eqn. 6 along with Eqns. 3 and 4 thus allows the plasma properties downstream of a cluster of identical Hall thrusters to be predicted based solely on measurements or simulations of a single unit. Results obtained in this way appear to be accurate to within the margin of error of typical plasma diagnostics.

$$\phi = \frac{k_B T_e}{e} \ln\left(\frac{n}{n_0}\right) \qquad (6)$$

As Figs. 16-20 show, the plasma potential profiles downstream of a cluster are fundamentally different than those of a single thruster. When ions exit a single Hall thruster, they experience a continuous decline in plasma potential as they proceed away from the device. In other words, the electric field vector is everywhere directed away

from the thruster. When multiple thrusters are operated together, however, a minimum in the plasma potential occurs in the region between the thrusters. This leads to a situation where sufficiently slow ions, such as those created by charge exchange (CEX), could be trapped in the potential well near the center of the cluster and reflected back upstream as mentioned previously. This situation is depicted in Fig. 21, below, where dashed blue lines represent equipotential contours in the reversed field region, i.e. in areas where the plasma potential increases with increasing downstream distance. The curved magenta line represents the path traversed by a low-energy, CEX ion created in the plume with insufficient kinetic energy to overcome the reversed electric field.

Fast ions, which comprise the majority of the discharge, would not be reflected by the relatively weak reversed electric field between the thrusters. They may, however, be deflected downstream by the plasma potential "hill" created by adjacent thrusters. This phenomenon is illustrated in Fig. 21, in which the blue lines represent contours of constant plasma potential and the red lines represent the trajectories of sample ions. The phenomenon illustrated in Fig. 21 may constitute an ion focusing mechanism by which ions initially directed toward the cluster center are deflected to marginally lower angles with respect to the cluster centerline. This effect may be responsible for the slightly reduced beam divergence reported by Hargus *et al.* for two operating thrusters compared to that predicted by linear superposition of the ion flux from individual thrusters.[8]

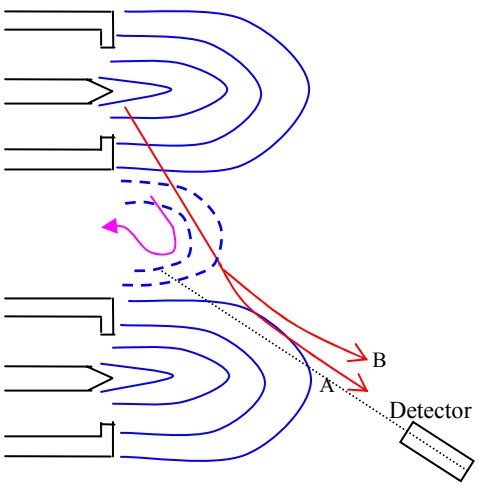

Figure 21: Ion focusing as a result of the plasma potential structure downstream of a cluster.

In addition to a possible reduction in overall beam divergence, the focusing mechanism discussed above may affect the ion energy spectra of Hall thruster clusters by preferentially deflecting low energy ions. One can gain insight into this mechanism by resorting to a simple phenomenological discussion. Consider two ions, A and B, exiting a thruster and traveling in an identical direction toward the center of the cluster, but with different initial kinetic energies. In this situation, the slower moving ion, B, would be deflected by a given potential rise to a greater degree than its high energy counterpart, ion A, as depicted in Fig. 21. Considering this, a detector swept through the plume would detect ion A at a higher angle off centerline, while ion B with its lower energy would be deflected further downstream and detected at a relatively low angle. This mechanism may be responsible for the low-energy structures visible in recently published ion energy data.[7]

Conclusion

A combination of triple Langmuir probes and floating emissive probes is used to characterize the plasma properties in the plume of a low-power Hall thruster cluster. The measurements show that the plasma density in the cluster plume can be predicted to a high level of accuracy by linear superposition of the density due to individual thrusters. The electron temperature downstream of a cluster of thrusters is slightly elevated compared to that measured downstream of a single thruster, although the change is modest and is within the level of uncertainty typical of the triple probe diagnostic. A reasonable estimate of the electron temperature profile in a cluster plume is obtained by calculating the density weighted average of the electron temperature due to each thruster operating individually. The plasma potential downstream of a cluster of Hall thrusters is shown to closely obey the Boltzmann relation.

Emissive probe measurements show a region between thrusters where the plasma potential increases with downstream distance. The unique potential profiles downstream of a cluster lead to a situation where low-energy charge exchange ions can be accelerated upstream by the weak, reversed electric fields that exist between thrusters. Fast ions initially directed toward the cluster centerline may be deflected downstream by various degrees depending on their energy to charge ratios. This ion focusing mechanism is hypothesized to be responsible for effects observed

in recently published ion flux and energy spectrum measurements.

References

1. Spanjers, G.G., *et al.*, "The USAF Electric Propulsion Research Program," AIAA-2000-3146, 36th Joint Propulsion Conference & Exhibit, Huntsville, AL, 2000.
2. Spores, R.A., *et al.*, "Overview of the USAF Electric Propulsion Program," AIAA-2001-3225, 37th Joint Propulsion Conference & Exhibit, Salt Lake City, UT, 2001.
3. Dunning Jr., J., *et al.*, "NASA's Electric Propulsion Program," IEPC-01-002, 27th International Electric Propulsion Conference, Pasadena, CA, 2001.
4. Dunning Jr., J., *et al.*, "NASA's Electric Propulsion Program," AIAA-2002-3557, 38th Joint Propulsion Conference & Exhibit, Indianapolis, IN, 2002.
5. http://spacescience.nasa.gov/missions/prometheus.htm
6. Beal, B.E., *et al.*, "Preliminary Plume Characterization of a Low-Power Hall Thruster Cluster," AIAA-2002-4251, 38th Joint Propulsion Conference & Exhibit, Indianapolis, IN, 2002.
7. Beal, B.E., *et al.*, "Energy Analysis of a Hall Thruster Cluster," IEPC-2003-0035, 28th International Electric Propulsion Conference, Toulouse, France, 2003.
8. Hargus Jr., W.A., *et al.*, "The Air Force Clustered Hall Thruster Program," AIAA-2002-3678, 38th Joint Propulsion Conference & Exhibit, Indianapolis, IN, 2002.
9. Hruby, V., *et al.*, "Development of Low Power Hall Thrusters," AIAA-99-3534, 30th Plasmadynamics and Lasers Conference, Norfolk, VA, 1999.
10. Haas, J.M., *et al.*, "Performance Characteristics of a 5 kW Laboratory Hall Thruster," AIAA-98-3503, 34th Joint Propulsion Conference & Exhibit, Cleveland, OH, 1998.
11. Haas, J.M., *et al.*, "Hall Thruster Discharge Characterization Using a High-Speed Axial Reciprocating Electrostatic Probe," AIAA-99-2430, 35th Joint Propulsion Conference & Exhibit, Los Angeles, CA, 1999.
12. Chen, S. and Sekiguchi, T., "Instantaneous Direct-Display System of Plasma Parameters by Means of Triple Probe," *Journal of Applied Physics*, **36**, 2363, 1965.
13. Tilley, D.L., *et al.*, "The Application of the Triple Probe Method to MPD Thruster Plumes," AIAA-90-2667, 21st International Electric Propulsion Conference, Orlando, FL, 1990.
14. Haas, J.M., *et al.*, "Characterization of the Internal Plasma Structure of a 5 kW Hall Thruster," IEPC-99-078, 26th International Electric Propulsion Conference, Kitakyushu, Japan, 1999.
15. Kemp, R.F. and Sellen Jr., J.M., "Plasma Potential Measurements by Electron Emissive Probes," *Review of Scientific Instruments*, **37**, 455, 1966.
16. Peterson, P.Y., *et al.*, "An Experimental Investigation of the Internal Magnetic Field Topography of an Operating Hall Thruster," *Physics of Plasmas*, **9**, 4354, 2002.
17. Manzella, D.H., "Stationary Plasma Thruster Ion Velocity Distribution," AIAA-94-3141, 30th Joint Propulsion Conference & Exhibit, Indianapolis, IN 1994.
18. Keidar M. and Boyd, I.D., "Effect of a Magnetic Field on the Plasma Plume from Hall Thrusters," *Journal of Applied Physics*, **86**, 4786, 1999.
19. Morozov, A.I., *et al.*, "Plasma Accelerator with Closed Electron Drift and Extended Acceleration Zone," *Soviet Physics – Technical Physics*, **17**, 38, 1972.